NUCLEAR SCIENCE AND ENGINEERING: 77, 157-167 (1981)

The Distribution of Thermal Neutron Cross Sections

Yu. V. Petrov and A. I. Shlyakhter

Leningrad Nuclear Physics Institute, Gatchina, Leningrad District 188350, USSR

Received August 13, 1979
Accepted May 29, 1980

An estimate of the cross sections of nuclear reactions with thermal neutrons in terms of the average parameters of the target nucleus (the strength function, the average level spacing, and the average reaction width) is obtained. The probability distributions for the ratios of actual thermal neutron cross sections to their estimated values are introduced. These functions can be calculated from the statistical model. They are calculated for neutron radiative capture and for inelastic neutron acceleration by the isomeric nuclei [as well as the (n,α) reaction, etc.]. Using these results, one can predict the probability of finding the actual thermal neutron cross section in a given interval.

I. INTRODUCTION

The capture cross sections for thermal neutrons [the (n,γ) reaction] have been measured for hundreds of nuclei.[1] However, for many nuclei (mainly unstable) they are still unknown. There are still fewer data on (n,α) thermal neutron cross sections[1,2] while thermal neutron cross section of the INelastic Neutron Acceleration (INNA reaction) by nuclear isomers was only recently first measured for ^{152m}Eu (Ref. 3). However, the need of estimating these cross sections in advance arises in a number of cases. One needs such estimates while planning the measurements of cross sections. They are also useful to estimate changes in the isotopic composition of the materials irradiated in nuclear reactors by a high neutron flux, etc.

At thermal energies, the cross section of a reaction is completely determined by the parameters of several low-lying resonances. These parameters vary significantly from one nucleus to another. Hence, even for the neighboring nuclei, cross sections can differ by several orders of magnitude and their exact values are unpredictable.

In the present paper, the thermal neutron cross section of each nucleus is considered as a random variable distributed about its estimated value. The latter is expressed in terms of the average parameters of this nucleus, such as the neutron strength function, the mean level spacing, and the average reaction width. All these quantities can be either calculated or measured at energies much greater than thermal. Then the distribution function for the ratio of the actual thermal neutron cross section to its estimated value is introduced. Within the limits of the statistical model, it is determined by the laws of the distribution of resonance parameters near the corresponding mean values. Hence, the distribution function is the same for similar reactions with nuclei having a given spin. Once calculated, this function can be used for the quantitative prediction of the probability that cross sections will deviate considerably from their expected values.

A similar function was first introduced by Gurevich[4] as long ago as 1939. It was used for estimating the mean level spacing between *s*-resonances in heavy nuclei. The actual distribution of the level spacings and the reduced neutron-width fluctuations had been unknown at that time. So, only the type of asymptotic behavior of the distribution function in the limit of very large cross sections had

[1]S. F. MUGHABHAB and D. I. GARBER, "Neutron Cross Sections," Vol. 1, "Resonance Parameters," BNL-325, 3rd ed., Brookhaven National Laboratory (1973).

[2]YU. P. POPOV, Preprint LNPI-267, Leningrad (1976); A. ANTONOV et al., Preprint JINR-P3-10372, Dubna (1977); (in Russian).

[3]YU. V. PETROV, *ZhETP (USSR)*, **37**, 1170 (1959); see also, *JETP (Sov. Phys.)*, **10**, 833 (1960); I. A. KONDUROV, E. M. KOROTKIKH, and YU. P. PETROV, *ZhETP, Pis'ma*, **31**, 254 (1980).

[4]I. I. GUREVICH, *ZhETF (USSR)*, **9**, 1283 (1939).

0029-5639/81/0002-0157$02.00/0

been established. However, it allowed Gurevich to arrive at an important conclusion about the sharp increase of the level density in the region of the rare earth nuclei.

In the region of unresolved resonances, Nikolaev and Filippov[5] and later Levitt[6] applied the probabilistic approach to the description of the cross-section energy dependence. However, their probability distributions are not universal, depending on the isotope and the energy interval considered.

In Sec. II we express the expected thermal neutron cross sections in terms of the mean values of the resonance parameters. In Sec. III the probability of the occurrence of large cross sections is considered and the distribution function $S(z)$ is introduced. Here, $S(z)$ is the probability of the ratio of the actual and estimated cross sections being less than z. In Sec. IV the capture cross-section distribution function $S_\gamma(z)$ is obtained analytically within the model of equidistant resonances. In Sec. V the fluctuations of the level spacings are taken into account using the Monte Carlo method. Our results are compared with the data on resonance parameters and capture cross sections for 105 nuclei from Refs. 1 and 7. This comparison confirms the validity of the latter model. In Sec. V we also consider the opposite case when the width of the exit channel obeys the Porter-Thomas distribution in the (n,α) reaction, the inelastic neutron acceleration by nuclear isomers, etc. The distribution functions, $S_{in}(z)$, similar to $S_\gamma(z)$, is obtained using the same model.

II. THE EXPECTED VALUES OF THERMAL NEUTRON CROSS SECTIONS

II.A. Basic Formulas

The contribution of a single resonance with spin J, energy E_i, neutron width Γ_{ni} and the exit channel width Γ_{ri}, to the reaction cross section is described by the Breit-Wigner formula as

$$\sigma_{ri} = \frac{\pi}{K^2}\frac{2J+1}{2(2I+1)}\frac{\Gamma_{ni}\cdot\Gamma_{ri}}{(E-E_i)^2+\left(\frac{\Gamma_i}{2}\right)^2}\,. \qquad (1)$$

Here,

$$K^2 = \left(\frac{A}{A+1}\right)^2\frac{2mE}{\hbar^2}$$

E = incident neutron energy in the laboratory system

A and I = atomic weight of the target nucleus and its spin.

At thermal energy, $E = E_T \equiv 0.0253$ eV, only the s-resonances contribute to the cross section, i.e., $J = I \pm \frac{1}{2}$. The inequalities $E_T \ll E_i$ and $\Gamma_i \ll E_i$ are usually true, so that Eq. (1) turns into

$$\sigma_{ri} = \frac{\pi}{K^2}\frac{2\left(I\pm\frac{1}{2}\right)+1}{2(2I+1)}\cdot\frac{\Gamma_{ni}\cdot\Gamma_{ri}}{E_i^2}\,. \qquad (2)$$

To estimate the cross-section value, let us represent it as the sum of the independent resonance contributions under the following simplifying assumptions:

1. All reaction widths are equal to the corresponding mean values (depending on J): $\Gamma_{ri} = \bar{\Gamma}_r(J)$, $\Gamma_{ni} = \bar{\Gamma}_n^0(J)(E/E_0)^{1/2}$, $E_0 = 1$ eV.
2. The energy spacings between the resonances with spin J are constant: $E_{i+1} - E_i = \bar{D}(J)$.
3. The resonances are located symmetrically with respect to the zero neutron energy point: $E_i = \bar{D}(J)(i-\frac{1}{2})$.

Using these assumptions, we come to the following expression for the expected cross-section value σ_r^*, which should not be confused with the mean value $\bar{\sigma}_r$:

$$\sigma_r^* = \frac{\pi}{K^2}\left(\frac{E}{E_0}\right)^{1/2}\left\{\frac{g(J_1)\cdot\bar{\Gamma}_n^0(J_1)\cdot\bar{\Gamma}_r(J_1)}{[\bar{D}(J_1)/2]^2} + \frac{g(J_2)\cdot\bar{\Gamma}_n^0(J_2)\cdot\bar{\Gamma}_r(J_2)}{[\bar{D}(J_2)/2]^2}\right\}\cdot\sum_{i=-\infty}^{\infty}\frac{1}{(2i-1)^2}\,. \qquad (3)$$

Here, $\bar{\Gamma}_n^0(J)$ is the mean neutron width, reduced to $E_0 \equiv 1$ eV, and $g(J) = (2J+1)/[2(2I+1)]$ is the statistical factor. The value of the sum in Eq. (3) is equal to $\pi^2/4$ (see Eq. 0.234.2 in Ref. 8).

II.B. The Expected Value of the Thermal Neutron Capture Cross Section

For the neutron capture reaction $\bar{\Gamma}_r(J) = \bar{\Gamma}_\gamma$, there are two systems of resonances (with spins $J_1 = I + \frac{1}{2}$ and $J_2 = I - \frac{1}{2}$) that give comparable contributions to the cross section. After substitution of the numerical factors corresponding to the thermal energy of the incident neutron ($E = E_T$), we obtain

$$\sigma_\gamma^* = 0.404\cdot 10^8\left(\frac{A+1}{A}\right)^2\cdot F(I)\cdot\frac{S_0\cdot\bar{\Gamma}_\gamma}{\bar{D}_{\exp}}\,\text{(b)}\,. \qquad (4)$$

Here,

$$F(I) = g^2(J_1) + g^2(J_2) = \frac{(I+1)^2+I^2}{(2I+1)^2}\,,$$

[5] M. N. NIKOLAEV and V. V. FILIPPOV, *Atomnaya Energia (USSR)*, **15**, 493 (1963).

[6] L. B. LEVITT, *Nucl. Sci. Eng.*, **49**, 450 (1972).

[7] W. DILG et al., *Nucl. Phys. A*, **217**, 269 (1973).

[8] I. S. GRADSTEIN and I. M. RYJIK, *Tables of Integrals, Sums, Series and Products*, 5th ed., Nauka, Moscow (1971).

$S_0 = \frac{g\bar{\Gamma}_n^0}{\bar{D}_{\exp}}$ = strength function for s-neutrons

$\bar{D}_{\exp}(I)$ = average spacing between s-resonances of the target nucleus with the spin I, which is connected with $\bar{D}(J)$ by the equality $\bar{D}_{\exp}(I) = g(J)\cdot\bar{D}(J)$.

For $I = 0$, Eq. (4) is reduced to

$$\sigma_\gamma^* = 0.404\cdot 10^8 \left(\frac{A+1}{A}\right)^2 \cdot \frac{S_0\cdot\bar{\Gamma}_\gamma}{\bar{D}_{\exp}} \text{ (b)} . \qquad (4a)$$

For example, let us estimate the capture cross section of thermal neutrons by the isomeric nucleus ^{152m}Eu ($I_g^\pi = 3^-$, $I_m^\pi = 0^-$, $\tau_g = 17.9$ yr. $\tau_m = 13.4$ h, $\epsilon_m = 0.05$ MeV, from Ref. 9). Vertebny et al.[10] obtained for the ground state of this nucleus $S_0 = (3.6 \pm 1.2)\cdot 10^{-4}$, $\bar{\Gamma}_\gamma = (0.160 \pm 0.025)$ eV, and $\bar{D}_{\exp}(3) = (0.25 \pm 0.04)$ eV. The evaluation of $\bar{D}_{\exp}$ for the spin of ^{152m}Eu using the Fermi gas model[11] gives $D_{\exp}(0) \approx 1.4$ eV. The values of S_0 and $\bar{\Gamma}_\gamma$ are spin independent. They should not change noticeably while the excitation energy is shifted by the isomer energy ϵ_m. Assuming them to be actually constant and using Eq. (4a), we obtain $\sigma_\gamma^* = 1.7\cdot 10^3$ b.

II.C. The Expected Value of the INNA Thermal Neutron Cross Section

We now consider the INNA reaction that is possible when the neutron collides with the isomeric nucleus.[3] As a result of the INNA reaction, the emitted neutron carries away the isomeric transition energy ϵ_m. Here, we consider only the magnetic-type isomers. In this case, the cross section is determined only by the system of resonances with spin corresponding to the lowest momentum of the emitted neutron. If we replace $\bar{\Gamma}_r$ by $\bar{\Gamma}_{in}(\epsilon_m)$ and take into account the approximate relation $\bar{\Gamma}_{in}(\epsilon_m)/\bar{\Gamma}_n^0 \approx T_{lj}(\epsilon_m)/T_0(E_0)$ [here, $T_{lj}(E)$ is the transmission coefficient for neutrons with the energy E, the orbital momentum l, and the total momentum j that are allowed by the selection rules of the transition], we have instead of Eq. (4),

$$\sigma_{in} = 0.404\cdot 10^8 \left(\frac{A+1}{A}\right)^2 \cdot g(J)\cdot S_0^2 \frac{T_{lj}(\epsilon_m)}{T_0(E_0)} \text{ (b)} . \qquad (5)$$

The transmission coefficients T_{lj} can be calculated using the optical model.

Let us use Eq. (5) to estimate the INNA thermal neutron cross sections for M4 isomers ^{87m}Sr, ^{113m}In, ^{115m}In, and ^{123m}Te. The important point here is the choice of reasonable parameters for the optical potential. In our earlier paper[12] we chose these parameters following the idea of the SPRT method by Lagrange.[13,14] The imaginary part of the potential W was obtained by fitting the strength function S_0, while other parameters were nearly those obtained by Lagrange for ^{89}Y and ^{93}Nb. The strength function S_1, the potential scattering radius R', and the total cross section $\sigma_t(E)$ were in reasonable agreement with the experimental data[1,15] [within 20% for S_1 and 10% for both R' and $\sigma_t(E)$]. This allowed us to describe the INNA cross section for ^{115m}In in the incident neutron-energy interval 0.02 to 0.3 MeV to an accuracy of ~20%. If we obtain the values of W for ^{87m}Sr, ^{113m}In, and ^{123m}Te in the same way, we arrive at σ_{in}^*, as listed in Table I.

This table shows that INNA cross sections, as a function of the isomer energy and of the strength function, can differ by orders of magnitude in spite of similar selection rules of the transition (M4). In particular ^{123m}Te must have a very small INNA cross section. The experimental limit $\sigma_{in} \leqslant 20$ mb established by Hamermesh[16] does not contradict our estimate.

III. THE PROBABILITY OF THE APPEARANCE OF LARGE CROSS SECTIONS

III.A. The Single Level Approximation

We now consider the distribution of the actual cross sections σ about their expected values σ^*. If we introduce the variable $z = \sigma/\sigma^*$ and consider it as random, we can define the probability density of z, $P(z)$, and the distribution function $S(z)$ as

$$S(z) = \int_0^z P(y)dy . \qquad (6)$$

Here, $S(z)$ is the probability that the ratio of the actual cross section to the expected one does not exceed z.

Let us suppose that some resonance is located occasionally quite near zero energy. Then the cross section is determined mainly by the parameters of this resonance and its actual value may greatly exceed the expected one. Thus, for large z the

[9] D. J. HOREN, Ed., *Nuclear Level Schemes*, Academic Press, Inc., New York (1973).

[10] V. P. VERTEBNY et al., *Yad. Fiz.*, **26**, 1137 (1977).

[11] A. BOHR and B. MOTTELSON, *Nuclear Structure*, Vol. 1, Benjamin, Inc., New York and Amsterdam (1969).

[12] YU. V. PETROV and A. I. SHLYAKHTER, *Nucl. Phys. A*, **292**, 88 (1977).

[13] CH. LAGRANGE, in *Proc. Third Sov. Natl. Conf. on Neutron Physics*, Kiev, May 26-30, 1975, CONF 750555, **3**, 65, Moscow (1976).

[14] J. P. DELAROCHE, CH. LAGRANGE, and J. SALVY, *Consultants' Mtg. Nuclear Theory in Neutron Nuclear Data Evaluation*, IAEA-190, **1**, 251, International Atomic Energy Agency (1976).

[15] D. I. GARBER and R. R. KINSEY, "Neutron Cross Sections," BNL-325, 3rd ed., Vol. 2, Brookhaven National Laboratory (1976).

[16] B. HAMERMESH, *Phys. Rev. C*, **10**, 2397 (1974).

TABLE I

Expected INNA Thermal Neutron Cross Sections

Isomer	$I_m^\pi \to I_g^\pi$	τ_m, h (Ref. 9)	ϵ_m, MeV (Ref. 9)	S_0, 10^{-4} (Ref. 1)	W_0, MeV	$\frac{T_{3\frac{1}{2}}(\epsilon_m)}{T_0(1\text{ eV})}$	σ, b
^{87m}Sr	$\frac{1^-}{2}\ \frac{9^+}{2}$	4.0	0.388	0.26	1.8	8.9	0.19
^{113m}In	$\frac{1^-}{2}\ \frac{9^+}{2}$	2.74	0.392	0.85	5.3	3.3	0.74
^{115m}In	$\frac{1^-}{2}\ \frac{9^+}{2}$	6.5	0.335	0.26	1.4	2.4	0.05
^{123m}Te	$\frac{11^-}{2}\ \frac{3^+}{2}$	$4.1\cdot10^3$	0.088	0.98	3.7	0.01	0.002

Note: Other parameters of the optical potential are those from Ref. 12. The values of V and W depend slightly on the incident neutron energy: $V = 49.5 - 0.28E$ (MeV), $W = W_0 + 0.3E$ (MeV).

asymptotic behavior of $P(z)$ and $S(z)$ is completely determined by the nearest resonance contribution and we can use the single level approximation. Taking into account Eqs. (2) and (3), we obtain for $I = 0$

$$z = \frac{4}{\pi^2}\cdot\frac{t\cdot u}{(v_0 - x)^2}\ . \tag{7}$$

Here, $t \equiv \Gamma_{n1}^0/\bar{\Gamma}_n^0$, $u \equiv \Gamma_{\gamma 1}^0/\bar{\Gamma}_\gamma^0$, and $v_0 \equiv (E_1 - E_0)/\bar{D}$ are, respectively, the reduced width of the first positive resonance and its spacing from the first negative level normalized to the corresponding mean values; $x \equiv -(E_0 + E_1)/\bar{D}$.

III.B. Probability Distributions of the Resonance Parameters

Within the framework of the statistical model, the fluctuations of the reduced widths are described by $\chi^2(\nu)$ distribution. The number of degrees-of-freedom ν is equal to the number of final states for the reaction considered.

There are only s-neutrons in the entrance channel; hence, $\nu = 1$ and the reduced neutron width should follow the Porter-Thomas distribution[11]:

$$P_{P\text{-}T}(t) = \frac{\exp(-t/2)}{(2\pi t)^{1/2}}\ . \tag{8}$$

The distribution of the reduced widths in the exit channel is determined by the type of the reaction. For radiative capture, there are a great number of final states. Hence, $\nu \gg 1$ and the $\chi^2(\nu)$ distribution is reduced to the delta function and one must put $u = 1$. In the opposite case, the compound nucleus decays into a single final state. Examples are the INNA reaction (the outgoing neutron has the lowest angular momentum allowed by the selection rules) and the (n,α) reaction (the compound nucleus decays preferably to the lowest level allowed). In the latter case, the Porter-Thomas distribution Eq. (8) agrees with the existing data.[2]

The fluctuations of the energy spacings between the neighboring levels with a given spin are usually described by a Wigner distribution[11] as

$$P_w(v_i) = \frac{\pi}{2}v_i\cdot\exp\left(-\frac{\pi}{4}v_i^2\right)\ . \tag{9}$$

Here, $v_i \equiv (E_{i+1} - E_i)/\bar{D}$.

The distribution of the energy of the first positive resonance is determined by the difference $(v_0 - x)/2$. It depends on the distribution of the incident neutron zero energy point on the scale of compound nucleus levels. It seems natural to suppose that the latter distribution is uniform. The total probability of finding the zero neutron energy in a given interval is proportional to its width v_0. The density function of the variable x is normalized to v_0 (due to the symmetry, one may consider only positive values of x):

$$P_0(x) = 1\ ,\quad 0 \leqslant x \leqslant v_0\ . \tag{10}$$

The validity of this density function is confirmed by the comparison of the theoretical distribution of the first resonance position with the available data (see Fig. 1 and Appendix A).

III.C. Distribution Functions in the Single Level Approximation

We now use the single level approximation to calculate the function $S(z)$ for a neutron radiative-capture reaction taking into account the distributions of Eqs. (8), (9), and (10). Denoting it by $S_\gamma(z)$ we have

$$S_\gamma^{(1)}(z) = \int_0^\infty dv_0\cdot P_w(v_0)\cdot\int_0^\infty du\cdot P_\gamma(u)\int_0^\infty dt \times P_{P\text{-}T}(t)\cdot\int_0^{v_0} dx\cdot P_0(x) \times\theta\left[z - \frac{4}{\pi^2}\frac{t\cdot u}{(v_0 - x)^2}\right]\ . \tag{11}$$

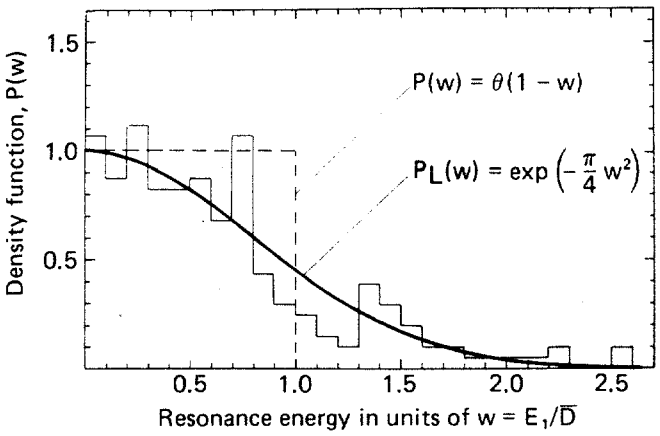

Fig. 1. The distribution of the first resonance energy (in units of $w \equiv E_1/\bar{D}$) with (solid line) and without (dashed line) the Wigner distribution of Eq. (9).

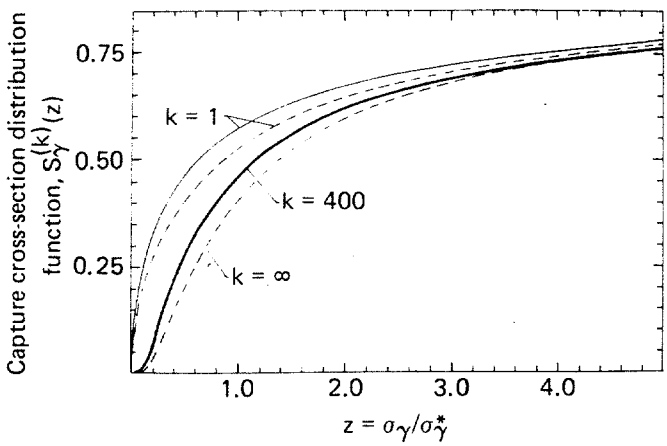

Fig. 2. The capture cross-section distribution function $S_\gamma^{(k)}(z)$ for zero spin nuclei with (solid line) and without (dashed line) the Wigner distribution of Eq. (9). Here, k is the number of resonances considered. In the case where $k = 400$, the Monte Carlo method was used.

Here, $\theta(x) = 1$, if $x \geqslant 0$; otherwise $\theta(x) = 0$. Integrating over x we come to

$$S_\gamma^{(1)}(z) = \int_0^\infty dv_0 \cdot P_w(v_0) \int_0^\infty du \cdot P_\gamma(u)$$

$$\times \int_0^{(\pi^2/4)(v_0^2/u)z} dt \cdot P_{P-T}(t) \cdot \left[v_0 - \frac{2}{\pi}\left(\frac{t \cdot u}{z}\right)^{1/2} \right] . \quad (12)$$

Evaluation of this integral finally gives

$$S_\gamma^{(1)}(z) = 1 - \frac{2}{\pi} \operatorname{arctg}\left(\frac{2}{\pi z}\right)^{1/2} . \quad (13)$$

At $z \gg 1$ the upper limit of the inner integral of Eq. (12) can be replaced by infinity and $S_\gamma^{(1)}$ is reduced to

$$S_\gamma^{(1)}(z) \approx \overline{(v_0)}_w - \frac{2}{\pi\sqrt{z}} \overline{(\sqrt{t})}_{P-T} \cdot \overline{(\sqrt{u})}_\gamma = 1 - \frac{2}{\pi}\left(\frac{2}{\pi z}\right)^{1/2} . \quad (14)$$

Here, $\overline{(v_0)}_w = 1$, $\overline{(\sqrt{t})}_{P-T} = (2/\pi)^{1/2}$, $\overline{(\sqrt{u})}_\gamma = 1$.

It is immediately seen from Eq. (12) that the rootlike asymptotic behavior of $S_\gamma(z)$ is due to the uniform distribution of the position of the first resonance [Eq. (10)]. The averaging of the neutron-width fluctuations in the entrance channel gives the factor $(2/\pi)^{1/2}$ while the distribution of resonance spacings does not change the asymptotics at all[17] (see case $k = 1$ in Fig. 2).

[17]It should be mentioned that the asymptotic formula similar to Eq. (14) can be derived from the expression obtained by Gurevich in 1939 (Ref. 4). He had neglected the fluctuations of the reduced neutron widths that were unknown at that time. Thus, in the limit of very large cross sections, his result can be reduced to the formula that differs from Eq. (14) by only the factor $(2/\pi)^{1/2}$.

The validity of the latter statement is illustrated in Fig. 1 where the distribution of the position of the first resonance (measured in $w \equiv E_1/\bar{D}$ units) with (solid line) and without (dashed line) Wigner distributions Eq. (9) is shown. At small w, the density function $P(w)$ does not depend on the model chosen. It means that at $z \gg 1$ the cross-section value is completely determined by the parameters of the nearest resonance and does not depend on the positions of the other resonances.

The single level approximation can also be used to obtain the function $S_{in}^{(1)}(z)$ for the INNA and the (n,α) reaction by substituting a Porter-Thomas distribution Eq. (8) instead of $p_\gamma(u)$ in Eq. (11). However, the result appears to be cumbersome and is not reproduced here (see case $k = 1$ in Fig. 3 and

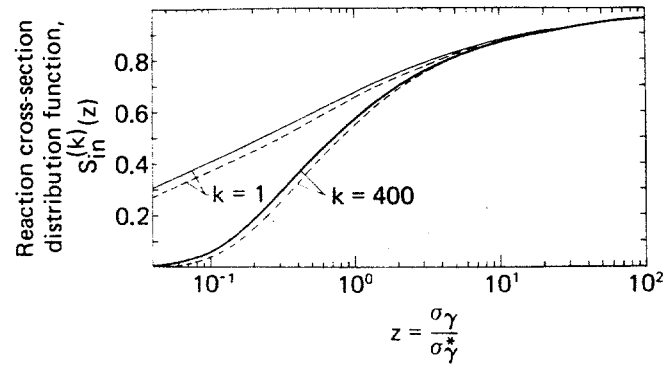

Fig. 3. The thermal INNA [as well as (n,α), etc.] reaction cross-section distribution function $S_{in}^{(k)}(z)$ with (solid line) and without (dashed line) the Wigner distribution of Eq. (9). Here, k is the number of resonances considered. In the case where $k = 400$, the Monte Carlo method was used.

Ref. 18). The asymptotic formula at large z can be obtained in the same way as Eq. (14)

$$S_{in} \approx \overline{(v_0)}_w - \frac{2}{\pi\sqrt{z}}\,\overline{(\sqrt{u})}_{P-T}\cdot\overline{(\sqrt{t})}_{P-T} = 1 - \frac{4}{\pi^2\sqrt{z}}\,. \tag{15}$$

It differs from Eq. (14) by an additional factor $(2/\pi)^{1/2}$, arising from the averaging of the width fluctuations in the exit channel.

III.D. Discussion

It follows from Eqs. (14) and (15) that the probability of large cross-section occurrence is not small and with the increase in z it decreases rather slowly (see Table II and Figs. 2 and 3). The thermal-capture cross section can exceed the expected value by more than 100 times with a probability of 5%. Almost 1% of the nuclei have capture cross sections that exceed their estimated values by more than a factor of $3\cdot10^3$. Thus, the existence of a number of strong absorbers is not surprising.

The probability of large INNA cross sections occurring is slightly smaller (by 20%) but still noticeable. For example Hamermesh[16] made an attempt to measure the INNA thermal neutron cross section for ^{123m}Te. The accuracy achieved was an order of magnitude less than that required (see Sec. II.C). However there existed a considerable probability (~13%) of measuring the effect; unfortunately it was not the case.

Let us note in conclusion that for very large z, the asymptotic formulas, Eqs. (14) and (15), should fail. This is due to the violation of the condition $\Gamma_1^2 \ll 4(E_1 - E_T)^2$ that allowed us to reduce Eq. (1) to Eq. (2). The corrections become significant at $z \approx \bar{D}^2/2\bar{\Gamma}^2$, which is usually large.

IV. DISTRIBUTION OF THE CAPTURE CROSS SECTIONS IN THE MODEL OF EQUIDISTANT RESONANCES

IV.A. Zero Spin of the Target Nucleus

As the nearest resonance is removed from zero neutron energy, its contribution to the cross section diminishes and one should take into account other resonances. We obtain the function $S_\gamma(z)$ within the framework of the following simple model. We suppose that the s-resonances form an equidistant system displaced an amount $\bar{D}$ on the energy axis. Thus, we replace the Wigner distribution Eq. (9) by

$$P(v_i) = \delta(v_i - 1)\,. \tag{16}$$

[18]YU. V. PETROV and A. I. SHLYAKHTER, Preprint LNPI-456, Leningrad (1979) (in Russian).

[19]The details of numerical calculations can be found in Ref. 18.

TABLE II

The Distribution Functions $S_\gamma(z)$ and $S_{in}(z)$

z	$S_\gamma(z)$[a]			$S_{in}(z)$[a]	z	$S_\gamma(z)$			$S_{in}(z)$
	0	$I_{1/2}$	∞			0	$I_{1/2}$	∞	
0.03				0.0006	0.50	0.27	0.30	0.30	0.42
0.04				0.003	0.60	0.32	0.35	0.35	0.46
0.05				0.007	0.70	0.37	0.39	0.40	0.50
0.06	0.001	0.001	0.001	0.015	0.80	0.40	0.42	0.43	0.53
0.07	0.002	0.002	0.002	0.024	0.90	0.43	0.45	0.46	0.55
0.08	0.003	0.004	0.004	0.035	1.0	0.46	0.48	0.49	0.57
0.09	0.006	0.006	0.006	0.046	1.5	0.56	0.58	0.58	0.65
0.10	0.009	0.010	0.010	0.059	2.0	0.62	0.63	0.63	0.70
0.12	0.017	0.020	0.020	0.085	2.5	0.66	0.67	0.67	0.73
0.14	0.028	0.032	0.032	0.11	3.0	0.69	0.70	0.70	0.75
0.16	0.040	0.046	0.047	0.14	3.5	0.72	0.72	0.72	0.77
0.18	0.054	0.062	0.063	0.16	4.0	0.74	0.74	0.74	0.79
0.20	0.070	0.079	0.081	0.19	4.5	0.75	0.76	0.76	0.80
0.25	0.11	0.12	0.12	0.24	5.0	0.77	0.77	0.77	0.81
0.30	0.14	0.16	0.17	0.28	10.0	0.83	0.83	0.83	0.87
0.35	0.18	0.20	0.20	0.32	20.0	0.88	0.88	0.88	0.91
0.40	0.22	0.24	0.24	0.36	50.0	0.93	0.93	0.93	0.94
0.45	0.25	0.27	0.27	0.39	100.0	0.95	0.95	0.95	0.96

[a]The distribution functions $S_\gamma(z)$ and $S_{in}(z)$ were calculated by the Monte Carlo method (Ref. 19). The contributions of 200 positive and 200 negative nearest resonances to the cross section were taken into account. For the calculation of each function, 10^5 sample cross sections were generated.

The energy of the i'th resonance is

$$E_i = \frac{\bar{D}}{2}(2i - 1 - x) \tag{17}$$

(in the notations of Sec. III). Here, i is an integer and x is the random variable, distributed uniformly in the interval $0 \leqslant x \leqslant 1$.

The contribution of the i'th resonance to the cross section is

$$y_i = \frac{4}{\pi^2}\frac{t_i}{(2i - 1 - x)^2} . \tag{18}$$

We calculate the probability density function using the Porter-Thomas distribution for the reduced neutron widths and neglecting the multilevel interference phenomena, and the fluctuations of the radiation widths (these are the usual approximations[20])

$$P_\gamma(z) = \int_0^1 dx \prod_{i=-\infty}^{\infty}\left[\int_0^\infty dt_i \cdot P_{P\text{-}T}(t_i)\right] \times \delta\left(z - \sum_{i'=-\infty}^{\infty} y_{i'}\right) . \tag{19}$$

Here, y_i are those defined in Eq. (18). The expression for the Laplace transform of the function $P_\gamma(z)$ is

$$\tilde{P}_\gamma(q) = \frac{4}{\pi}\operatorname{arctg}\exp[-(2q)^{1/2}] . \tag{20}$$

Equation (20) is derived in Appendix B. It leads to

$$P_\gamma(z) = \frac{2}{\pi^2}\int_0^\infty \exp\left(\frac{-y^2 z}{2}\right)\cdot \operatorname{Arth}(\sin y)dy . \tag{21}$$

For small q lying within the circle $|q| < \pi^2/8$, $\tilde{P}_\gamma(q)$ can be developed as a series in $(2q)^{1/2}$. The inversion of each of its terms gives us the asymptotic expansion for large z:

$$P_\gamma(z) = \frac{2}{\pi}\left(\frac{2}{\pi z}\right)^{1/2}\sum_{n=0}^{\infty}\frac{|E_{2n}|}{n!(2z)^{n+1}} = \left(\frac{2}{\pi z^3}\right)^{1/2}\left(1 + \frac{1}{6z} + \frac{1}{8z^2} + \ldots\right) . \tag{22}$$

Here, E_{2n} are the Euler numbers $E_0 = 1$, $E_2 = -1$, $E_4 = 5$, $E_6 = -61$, $E_8 = 1385\ldots$ (see Secs. 9.63 and 9.72 in Ref. 8). Hence,

$$S_\gamma(z) = 1 - \frac{2}{\pi}\left(\frac{2}{\pi z}\right)^{1/2}\left(1 + \frac{1}{6z} + \frac{1}{8z^2} + \ldots\right) . \tag{23}$$

This expression gives the accuracy of the single level approximation of Eq. (14).

[20] G. de SAUSSURE and R. B. PEREZ, *Nucl. Sci. Eng.*, **52**, 382 (1973).

It is inconvenient to use Eqs. (22) and (23) at small z. After developing the arc tangent in Eq. (20) as a power series in $\exp[-(2q)^{1/2}]$ and inverting each term, we obtain

$$P_\gamma(z) = \left(\frac{2}{\pi z}\right)^{3/2}\cdot\sum_{n=0}^{\infty}(-1)^n\cdot\exp\left[-\frac{(2n+1)^2}{2z}\right] . \tag{24}$$

This series converges rapidly for small z and the following approximation has an accuracy of better than 2% up to $z = 1$:

$$P_\gamma(z) \approx \left(\frac{2}{\pi z}\right)^{3/2}\exp\left(-\frac{1}{2z}\right) . \tag{24a}$$

The fast decrease of $P_\gamma(z)$ at $z \to 0$ is due to the fact that z can become small only if the widths of the large number of resonances become small simultaneously. The function Eq. (24a) reaches its maximum value at $z_m = \frac{1}{3}$, i.e., $P_\gamma(z_m) = 0.589$. The plot of the function $P_\gamma(z)$ is shown in Fig. 4. After integration of Eq. (24) from zero to z, we obtain the expression for $S_\gamma(z)$, which is convenient at small z:

$$S_\gamma(z) = \frac{4}{\pi}\sum_{n=0}^{\infty}\frac{(-1)^n}{(2n+1)}\operatorname{erfc}\left[\frac{2n+1}{(2z)^{1/2}}\right] . \tag{25}$$

Hence,

$$S_\gamma(z) \underset{z\to 0}{\approx} \frac{4}{\pi}\left(\frac{2}{\pi}z\right)^{1/2}\cdot\exp\left(-\frac{1}{2z}\right) . \tag{25a}$$

The function $S_\gamma(z)$ is shown in Fig. 2. As was expected, it differs significantly from the single level approximation used in Sec. III at small z.

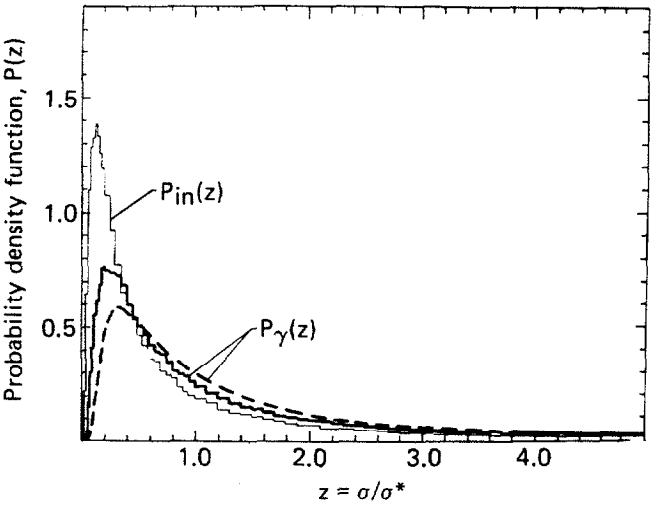

Fig. 4. The probability density functions $P_\gamma(z)$ and $P_{in}(z)$ for thermal neutron cross sections with (solid line, the Monte Carlo calculation) and without (dashed line) the Wigner distribution of Eq. (9).

IV.B. Arbitrary Spin of the Target Nucleus

It is convenient to take the expected capture cross section for $I = 0$ [Eq. (4a)] as a unit. The contributions of the systems of equidistant resonances with the spins $J_1 = (I + \frac{1}{2})$ and $J_2 = (I - \frac{1}{2})$ are proportional to $g_1^2 = (I + 1)^2/(2I + 1)^2$ and $g_2^2 = I^2/(2I + 1)^2$, respectively.

Assuming both systems to be independent, we have for the Laplace transform of the distribution function

$$\tilde{S}_\gamma(q) = \left(\frac{4}{\pi}\right)^2 \frac{1}{q} \operatorname{arctg} \exp[-g_1(2q)^{1/2}] \operatorname{arctg} \times \exp[-g_2(2q)^{1/2}] \ . \quad (26)$$

Equation (26) is derived in Appendix B. We develop $\operatorname{arctg}\{\exp[-g_K(2q)^{1/2}]\}$ as a power series in $\exp[-g_K(2q)^{1/2}](k = 1, 2)$ and invert it term by term just as in the case of $I = 0$:

$$S_\gamma(z) = \left(\frac{4}{\pi}\right)^2 \cdot \sum_{n=0}^{\infty} \sum_{m=0}^{n} \frac{(-1)^n}{(2n+1)(2n-2m+1)} \times \operatorname{erfc}\left[\frac{(2n+1)g_1 + (2n-2m+1)g_2}{(2z)^{1/2}}\right] \ . \quad (27)$$

This expression is convenient at small z. For $z \ll 1$ we have

$$S_\gamma(z) \underset{z\to 0}{\approx} \left(\frac{4}{\pi}\right)^2 \left(\frac{2}{\pi} z\right)^{1/2} \exp\left(-\frac{1}{2z}\right) \ . \quad (27a)$$

The comparison of Eqs. (27) and (27a) shows that spin causes the appearance of the pre-exponential factor $4/\pi = 1.27$.

In the opposite case (large z) the following expression is valid for $P_\gamma(z)$:

$$P_\gamma(z) \approx \frac{2}{\pi^2} \int_0^\infty \left[\exp\left(-\frac{y^2 z}{2g_1^2}\right) + \exp\left(-\frac{y^2 z}{2g_2^2}\right)\right] \times \operatorname{Arth}(\sin y) \cdot y \cdot dy \ , \quad z \gg \frac{8g_2^2}{\pi^2} \ . \quad (28)$$

Hence, Eqs. (21), (22), and (23) give us

$$S_\gamma(z) = 1 - \int_z^\infty P_\gamma(y)dy \approx 1 - \frac{2}{\pi}\left(\frac{2}{\pi z}\right)^{1/2} \sum_{n=0}^{\infty} \frac{|E_{2n}|(g_1^{2n+1} + g_2^{2n+1})}{(2n+1) \cdot n! (2z)^n} \ . \quad (29)$$

Unlike the expansions (21) and (23), which are exactly equal to Eqs. (24) and (25), Eqs. (28) and (29) are valid only at $z \gg 8g_2^2/\pi^2$ with the exponential accuracy.

Comparison of Eqs. (29) and (23) show that the spin influence appears only in the second term of the expansion as

$$S_\gamma(z) = 1 - \frac{2}{\pi}\left(\frac{2}{\pi z}\right)^{1/2}\left(1 + \frac{g_1^3 + g_2^3}{6z} + \frac{g_1^5 + g_2^5}{8z^2} + \ldots\right) \quad (29a)$$

and at large z the spin corrections are small. Thus, in the model of equidistant resonances, a small correction at large z and a factor 1.27 at small z appear to be due to spin. The direct calculation shows that the influence of spin is small at all z. A more accurate treatment confirms this conclusion (see Sec. V).

V. THE INFLUENCE OF THE LEVEL SPACING FLUCTUATIONS

V.A. The Capture Reaction

The fluctuations of the level spacings change the distribution of the cross sections. As was shown in Sec. III at $z \gg 1$, these fluctuations do not influence the asymptotics of $S_\gamma(z)$. In the region $z \ll 1$, the cross section is determined by the parameters of many resonances. Therefore, there is a possibility that the cross section will decrease due to the increase of the level spacings. This effect slows the rapid decrease of $S_\gamma(z)$. The exact analytical solution was not obtained in this case. However, the direct Monte Carlo simulation of the cross sections by means of a computer proved sufficient. Figure 2 shows the functions $S_\gamma(z)$ for $I = 0$ that were calculated with (solid line) and without (dashed line) the Wigner distribution of the level spacings. Apparently the accuracy of the model of equidistant resonances decreases quickly while $z \to 0$.

The influence of the level spacings fluctuations on the function $P_\gamma(z)$ at $z \lesssim 1$ is shown in Fig. 4. This function reaches its upper limit at $z = z_m$; here, z_m is ~1.5 times less than in the model of equidistant resonances while the maximum value is higher. Thus, the most probable capture cross section is almost one-fifth the expected value, σ_γ^*, calculated using Eq. (4a). (The scatter of points due to the Monte Carlo calculation prevents the exact determination of z_m.)

The probability of very small values of z is negligible (see Figs. 2 and 4 and Table II): $S_\gamma(z) \leqslant 10^{-3}$ at $z \leqslant 0.05$. So, one can neglect the probability of the cross section being 20 (or more) times less than σ_γ^* and thus can establish the lower limit on possible values of σ_γ.

V.B. INNA Reaction

Here, we consider the case of the compound nucleus decay into a single final state. Now the widths of both the initial and final channel obey the Porter-Thomas distribution [INNA reaction, (n,α), etc.]. We calculated the function $P_{in}(z)$ taking into account the Wigner distribution. The Monte

Carlo method was used. The results are shown in Fig. 4. The upper limit of $P_{in}(z)$ is considerably higher and it is shifted to the left compared to $P_\gamma(z)$. The most probable cross-section value appears to be about eight times less than σ^*_{in} within the accuracy of the calculation.

The influence of the level spacings fluctuations can be seen in Fig. 3 where the functions $S_{in}(z)$ calculated with and without the Wigner distribution are shown. This influence appears to be less important than in the case of $S_\gamma(z)$ (see Fig. 2).

The probability of small z is considerably greater for the INNA reaction than for capture as one can see in Fig. 4 and Table II. However, the values less than $z = 0.03$ are hardly probable and one can adopt it as a lower limit of z.

V.C. The Data Analysis

The calculated values of $S_\gamma(z)$ are compared with data in Fig. 5. We have already noted that the calculated curves at the target nucleus spin values $I = 0$ and $I \neq 0$ are close to one another. The influence of spin is less than in the model of equidistant resonances. The difference between $S_\gamma(z)$ for $I = \frac{1}{2}$ and $I = \infty$ is not more than the thickness of the curve $I \neq 0$ (see also Table II).

We have included in the data set the nuclei for which both the thermal neutron capture cross sections and the parameters of several lowest s-resonances were known. Having the ratio $z_{exp} = \sigma_{\gamma exp}/\sigma^*_\gamma$ for each nucleus, one can plot a histogram for $S_{\gamma exp}(z)$. Such a histogram based on the data for 105 nuclei $45 \leqslant A \leqslant 240$ (41 nuclei have zero spin) from Refs. 1 and 7 is shown in Fig. 5. All the nuclei (not fissionable in the thermal region), for which the parameters in Eq. (4a) could be determined reliably enough, were included.

The agreement between our calculations and the experimental data is quite satisfactory. In the region $z \gg 1$, it confirms the purely random distribution of the zero neutron energy on the scale of nuclear levels. The agreement in asymptotic behavior also confirms the validity of the Porter-Thomas distribution Eq. (8) [see the discussion of Eq. (14) in Sec. III]. At $z \lesssim 1$ the agreement with the data can be reached by taking into account only the latter distribution and the one of Wigner, Eq. (9). Within the accuracy of the data available, one can neglect possible deviations from these purely statistical distributions as well as the possible multilevel interference phenomena.

There are no experimental data to verify the function $S_{in}(z)$. However, it was obtained within the same model. The interference phenomena can appear to be more important in this case.[20] Nevertheless, we can recommend it for estimating the probability of the considerable deviations of thermal INNA cross sections [as well as (n,α), etc.] from their expected values.

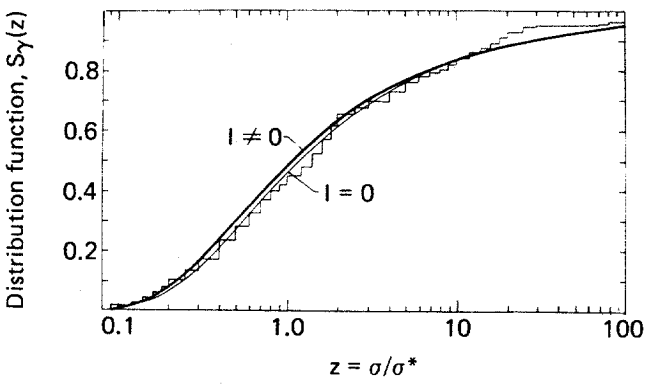

Fig. 5. Comparison of the calculated distribution functions $S_\gamma(z)$ (depending on the target nucleus spin I) with the experimental data from Refs. 1 and 7. The data set includes 105 nuclei with $45 \leqslant A \leqslant 240$.

V.D. Conclusion

It appears convenient to consider actual thermal neutron cross sections as random variables distributed about their estimated values. Equations (4a) and (5), taken with the corresponding distribution functions (see Figs. 3 and 5 and Table II), allow prediction of the probability of various cross-section values.

The probability of small values of $z \equiv \sigma_{exp}/\sigma^*$ is exponentially small. Thus, the lower limit of the possible cross-section values can be established reliably enough. On the other hand, the probability of the occurrence of the cross sections by orders of magnitude exceeding their expected values is noticeable.

The agreement of the calculated distribution function for capture $S_\gamma(z)$ with the experimental data (see Fig. 5) indicates that the statistical approach can be used both for resonance parameters and thermal cross sections. This seems to be an independent confirmation of the statistical model.

APPENDIX A

In this Appendix we verify the hypothesis that the zero energy of the incident neutron is located in a purely random way with respect to the compound nucleus levels scale.

In the statistical model, it is generally assumed that the levels of the excited nucleus are scattered near the neutron emission threshold in such a way that spacings between the neighboring resonances obey the Wigner distribution, Eq. (9). If the neutron zero energy can enter any point of the energy scale with equal probability, then the chance to enter a given interval is proportional to its width v_0. Inside

this interval, the zero neutron energy is distributed with uniform probability and $P_0(x) = \frac{1}{2}$, being independent on the first negative level position. The distribution $P_0(x)$ is still normalized to v_0, but unlike Eq. (10) the possibility of x variation in both directions must be considered ($-v_0 \leqslant x \leqslant v_0$).

Let us obtain the probability density of the first resonance position $w = (v_0 - x)/2$. It is determined by the difference of the two independent random numbers v_0 and x following $P_w(v_0)$ and $P_0(x)$ distributions. Hence,

$$P_L(w) = \int_0^\infty dv_0 \cdot P_w(v_0) \int_{-v_0}^{v_0} dx \cdot P_0(x) \times \delta\left(w - \frac{v_0 - x}{2}\right) = \exp\left(-\frac{\pi}{4} w^2\right) . \quad (A.1)$$

The $P_L(w)$ distribution was obtained in 1968 by Lynn[21] in connection with the problem of the possible nonstatistical effect in the distribution of the neutron emission thresholds. Lynn compared the $P_i(w)$ distribution with the data and satisfactory agreement was found. Since the new data appeared during the last years, it seems reasonable to repeat the comparison with the improved statistics.

All the nuclei with known spin of the first-resonance and mean spacing between the s-resonances[1,7] were included in our analysis. The level systems with $J_1 = I + \frac{1}{2}$ and $J_2 = I - \frac{1}{2}$ were analyzed independently. The final data set contained 206 points (instead of the 60 points in Ref. 21).

The experimental histogram is shown in Fig. 1. The probability densities $P(w)$ were calculated both with (solid line) and without (dashed line) the Wigner distribution. The good agreement of the Lynn distribution with the experiment confirms the hypothesis on the random distribution of the incident neutron zero energy with respect to the compound nucleus levels.

In the region of small w, the Wigner distribution does not change the result obtained in the model of equidistant resonances noticeably, the difference becoming significant only at $w \approx 1$. The existing agreement of $P_L(w)$ distribution with the data gives an additional support to the Wigner distribution of Eq. (9). It should be emphasized that here the statistical approach was applied to the totality of the resonances of many nuclei, not of a single nucleus.

APPENDIX B

LAPLACE TRANSFORM OF THE FUNCTION $S_\gamma(z)$ IN THE MODEL OF EQUIDISTANT RESONANCES

Let us consider the target nucleus with zero spin I. In accordance with Eq. (19), the function $P_\gamma(z)$ can be represented as

$$P_\gamma(z) = \int_0^1 dx \prod_{i=-\infty}^{\infty} \left[\int_0^\infty dt_i \cdot P_{P-T}(t_i)\right] \times \delta\left[z - \sum_{i'=-\infty}^{\infty} y_{i'}(t_{i'})\right] . \quad (B.1)$$

Carrying out the Laplace transformation and changing the order of integrations, we obtain

$$\tilde{P}_\gamma(q) \equiv \int_0^\infty \exp(-qz) \cdot P_\gamma(z) dz = \int_0^1 dx \prod_{i=-\infty}^{\infty} \left\{\int_0^\infty dt_i \cdot \exp[-y_i(t_i)] \cdot P_{P-T}(t_i)\right\} . \quad (B.2)$$

Calculating the inner integrals and taking into account Eqs. (8) and (18), we obtain

$$\tilde{P}_\gamma(q) = \int_0^1 dx \prod_{i=-\infty}^{\infty} \frac{1}{\left[1 + \frac{8}{\pi^2} \frac{q}{(2i - 1 - x)^2}\right]^{1/2}} . \quad (B.3)$$

For this infinite product, the following formula is valid (see Eq. 1.438 in Ref. 8):

$$\prod_{i=-\infty}^{\infty} \left[1 + \frac{8}{\pi^2} \frac{q}{(2i - 1 - x)^2}\right] = \frac{ch(8q)^{1/2} + \cos\pi x}{1 + \cos\pi x} . \quad (B.4)$$

Substituting Eq. (B.4) into Eq. (B.3) and integrating over x, we obtain finally the Laplace transforms of $P_\gamma(z)$ and $S_\gamma(z)$:

$$\tilde{P}_\gamma(q) = \frac{4}{\pi} \operatorname{arctg} \exp[-(2q)^{1/2}]$$

$$\tilde{S}_\gamma(q) = \frac{4}{\pi q} \operatorname{arctg} \exp[-(2q)^{1/2}] . \quad (B.5)$$

In the case of the arbitrary spin of the target nucleus, the contribution of the i'th resonance belonging to the k'th system differs from Eq. (18) by the factor g_K^2:

$$y_{iK} = g_K^2 \cdot \frac{4}{\pi^2} \frac{t_i}{(2i - 1 - x)^2} , \quad k = 1, 2 . \quad (B.6)$$

Assuming both systems to be independent we have, instead of Eq. (B.1),

[21] J. E. LYNN, *The Theory of Neutron Resonance Reactions*, Oxford (1968).

$$P_\gamma(z) = \left\{ \int_0^1 dx_1 \prod_{i=-\infty}^{\infty} \left[\int_0^\infty dt_i \cdot P_{P-T}(t_i) \right] \right\}$$

$$\times \left\{ \int_0^1 dx_2 \cdot \prod_{j=-\infty}^{\infty} \left[\int dt_j \cdot P_{P-T}(t_j) \right] \right\}$$

$$\times \delta \left[z - \sum_{i'=-\infty}^{\infty} y_{i'1}(t_{i'}) - \sum_{j'=-\infty}^{\infty} y_{j'2}(t_{j'}) \right] . \quad \text{(B.7)}$$

Just as in the case $I = 0$, we obtain

$$\tilde{P}_\gamma(q) = \left(\frac{4}{\pi}\right)^2 \cdot \operatorname{arctg} \exp[-g_1(2q)^{1/2}]$$

$$\times \operatorname{arctg} \exp[-g_2(2q)^{1/2}]$$

$$\tilde{S}_\gamma(q) = \left(\frac{4}{\pi}\right)^2 \frac{1}{q} \operatorname{arctg} \exp[-g_1(2q)^{1/2}]$$

$$\times \operatorname{arctg} \exp[-g_2(2q)^{1/2}] . \quad \text{(B.8)}$$

Note Added in Proof: After this work was completed, we learned about the paper by Cook and Wall.[22] They used data on the position of the first resonance and Monte Carlo method for generating probability distributions of thermal capture cross sections around estimated values. No exact analytical solution was obtained.

ACKNOWLEDGMENTS

We are indebted to E. A. Garusov, V. Yu. Petrov, and Yu. M. Shabelsky for their valuable comments.

[22] J. L. COOK and A. L. WALL, *Nucl. Sci. Eng.*, **31**, 234 (1968).